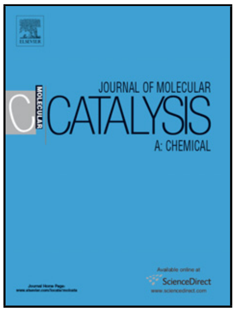

Title: An immobilized imidazolyl manganese porphyrin for the oxidation of olefins

Author: Rodrigo De Paula Isabel C.M.S. Santos Mário M.Q. Simõ es M.Graça P.M.S. Neves José A.S. Cavaleiro

PII: S1381-1169(15)00171-5
DOI: http://dx.doi.org/doi:10.1016/j.molcata.2015.04.021
Reference: MOLCAA 9484

To appear in: *Journal of Molecular Catalysis A: Chemical*

Received date: 17-12-2014
Revised date: 28-3-2015
Accepted date: 27-4-2015

Please cite this article as: Rodrigo De Paula, Isabel C.M.S.Santos, Mário M.Q.Simõ es, M.Graça P.M.S.Neves, José A.S.Cavaleiro, An immobilized imidazolyl manganese porphyrin for the oxidation of olefins, Journal of Molecular Catalysis A: Chemical http://dx.doi.org/10.1016/j.molcata.2015.04.021

An immobilized imidazolyl manganese porphyrin for the oxidation of olefins

Rodrigo De Paula[§], Isabel C. M. S. Santos, Mário M. Q. Simões, M. Graça P. M. S. Neves[*], José A. S. Cavaleiro[*]

QOPNA, Department of Chemistry, University of Aveiro, 3810-193 Aveiro, Portugal

[*]Corresponding Authors

Professor Dr. M. Graça P. M. S. Neves

Phone: +351 234 370 710; Fax: +351 234 370 084; E-mail: gneves@ua.pt

Professor Dr. José A. S. Cavaleiro

Phone: +351 234 370 717; Fax: +351 234 370 084; E-mail: jcavaleiro@ua.pt

[§]Present Address: Universidade Federal do Recôncavo da Bahia – Centro de Formação de Professores, 45.300-000 Amargosa/BA – Brazil, Tel: +55 75 3634 3042, Fax: +55 75 3634 3703); e-mail: rodrigodepaula@ufrb.edu.br

---

Graphical Abstract

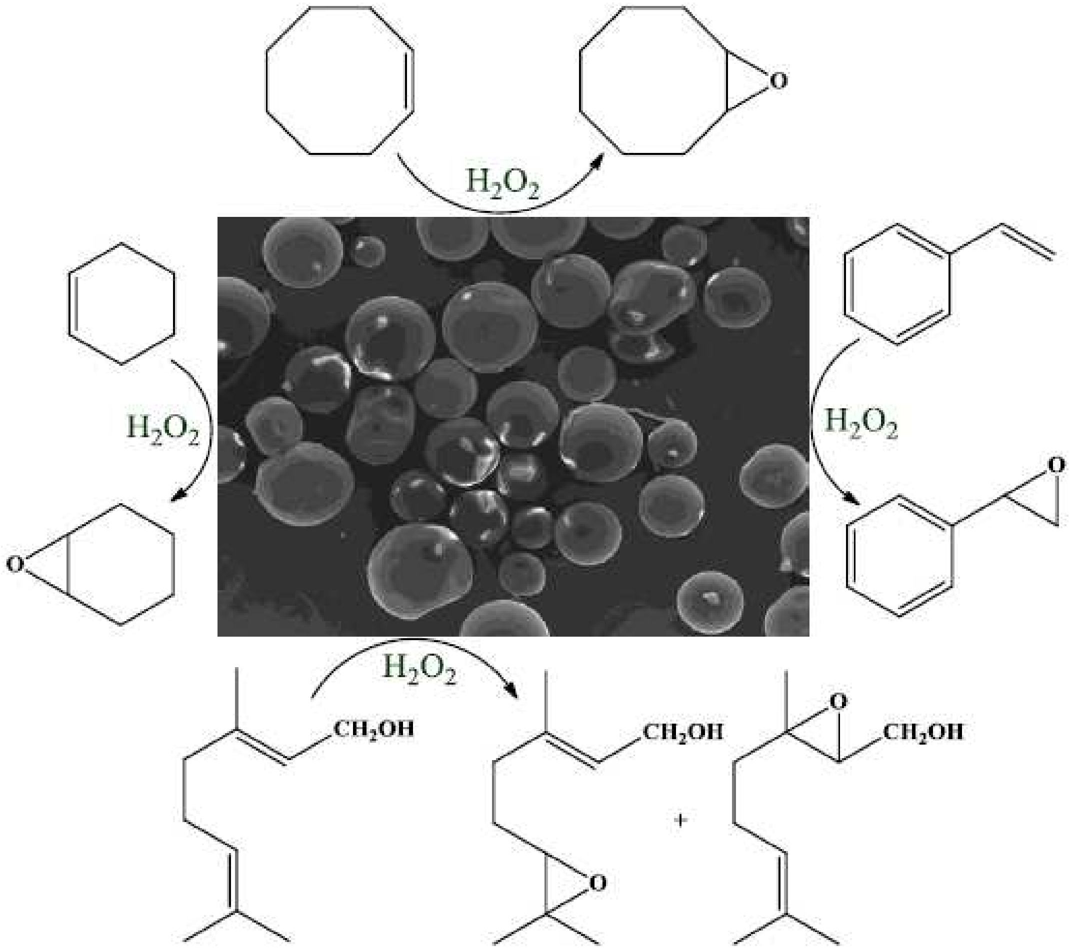

Highlights

- A new catalytic system based on an immobilized imidazolyl manganese porphyrin.
- Merrifield resin (**MR**) and functionalized silica gel (**SG**) as supports.
- **MR** system shows high reaction rates, high efficiency and good recyclability.
- Very high selectivity for cyclooctene, styrene, cyclohexene and geraniol epoxides.

Abstract

A new catalytic system based on an immobilized imidazolyl manganese porphyrin for the oxidation of olefins is presented. Merrifield resin (**MR**) and functionalized silica gel (**SG**) were chosen as supports. The results indicate that the **MR** system shows high reaction rates, high efficiency with hydrogen peroxide as oxidant and good recyclability up to four times, without a dramatic loss in the catalytic efficiency. The catalytic behavior seems to be strongly influenced by the immobilization reaction conditions. The oxidation reactions performed for *cis*-cyclooctene, styrene, cyclohexene and geraniol give the corresponding epoxides, with very high selectivity, when the **MR** system is used. Some considerations concerning the high efficiency of the **MR** system are put forward.

KEYWORDS: manganese(III)porphyrin; *tert*-butylhydroperoxide; hydrogen peroxide; Merrifield resin; functionalized silica; oxidation.

1. INTRODUCTION

Metalloporphyrins are widely used as catalysts in oxidation reactions,[1-3] mimicking the natural functions performed by cytochrome P450 monooxygenase enzymes.[4-7] The natural system is constituted by an iron porphyrin surrounded by proteins which is capable of selectively catalyze the oxidation and, in particular, the epoxidation of a wide range of substrates.[8-10] Iron is the “workhorse” in many biological processes and, concerning the *monooxygenases*, iron drives the oxidation of many substrates by mechanistic routes involving a hypervalent oxo-species.[9,11-18] Like iron, manganese also forms a high-valent oxo intermediate that can promote the oxidation of many substrates,[19-21] and manganese complexes are often preferred for biomimetic *in vitro* catalysis, due to their higher activity.[9,10]

There are a lot of reports concerning metalloporphyrins catalyzed oxidation under homogeneous conditions.[9,10,21-34] However, the synthesis of metalloporphyrins is a challenging task and usually a low yielding process. Also the known instability of these catalysts towards oxidative degradation and the difficulty in their recovery can limit the putative practical applications of metalloporphyrins as catalysts in both laboratory synthetic chemistry and industrial processes. On the other hand, immobilization of metalloporphyrin complexes on solid supports can provide catalysts easier to handle, that may exhibit improved selectivity and activity due to the support environment.[35-40] To date, different approaches have been developed for the design of heterogeneous metalloporphyrin catalysts, including: (i) electrostatic binding of charged porphyrins to counter-charged supports; (ii) intercalation or entrapment of porphyrins between the layers of clays or within the pores or matrices of solids; (iii) axial anchoring to surface-bound ligands; and (iv) covalent binding to appropriate supports. Recently, our group was able to develop two immobilized systems, one using a manganese complex of 5,10,15,20-tetrakis(2,6-dichlorophenyl)porphyrin[41] and the other based on the corresponding chlorin.[42]

Differently from the well-studied *meso*-phenyl substituted porphyrins, we have recently published the use of an imidazolium-based tetracationic manganese porphyrin as catalyst under homogeneous conditions.[12,24] The neutral parent of that catalyst, the manganese complex of 5,10,15,20-tetrakis(1-methylimidazol-2-yl)-21*H*,23*H*-porphyrin [**Mn(Porph)]** did not exhibit a great catalytic activity in homogeneous media; however, when linked to a solid support, a great improvement is observed. This paper deals with the experimental results obtained for the imidazolyl-based manganese porphyrin covalently bound to two distinct solid supports, the 3-bromopropylfunctionalized silica gel and the Merrifield resin (Figure 1) in the epoxidation of *cis*-cyclooctene. This support selection was based on the fact that the 3-bromopropylsilica and the Merrifield resin allow, by a simple nucleophilic substitution reaction, to covalently anchor the metalloporphyrin, instead of other systems where the immobilization lies on support/metal interactions or through support/macrocycle electrostatic interactions.

The most promising **Mn(Porph)-MR** heterogeneous catalyst was also tested for styrene, cyclohexene and geraniol oxidation and the results are also presented here.

2. RESULTS AND DISCUSSION

2.1. Synthesis and Characterization

Some previous results showed that the neutral manganese(III) complex of 5,10,15,20-tetrakis(1-methylimidazol-2-yl)-21*H*,23*H*-porphyrin has extremely low catalytic activity.[11] However, once positively charged, its activity changes dramatically reaching high conversion and high selectivity to epoxide for many olefins.[24] In this way, we have decided to attach the metalloporphyrin into a solid support, in order to obtain a positively charged and immobilized material, simultaneously. The different experimental procedures used to immobilize the **Mn(Porph)** in the two supports selected, the Merrifield resin (**MR**) and the 3-bromopropylfunctionalized silica gel (**SG**), are summarized in Scheme 1; these conditions were adapted from a procedure reported by Tangestaninejad *et al.*.[36,43]

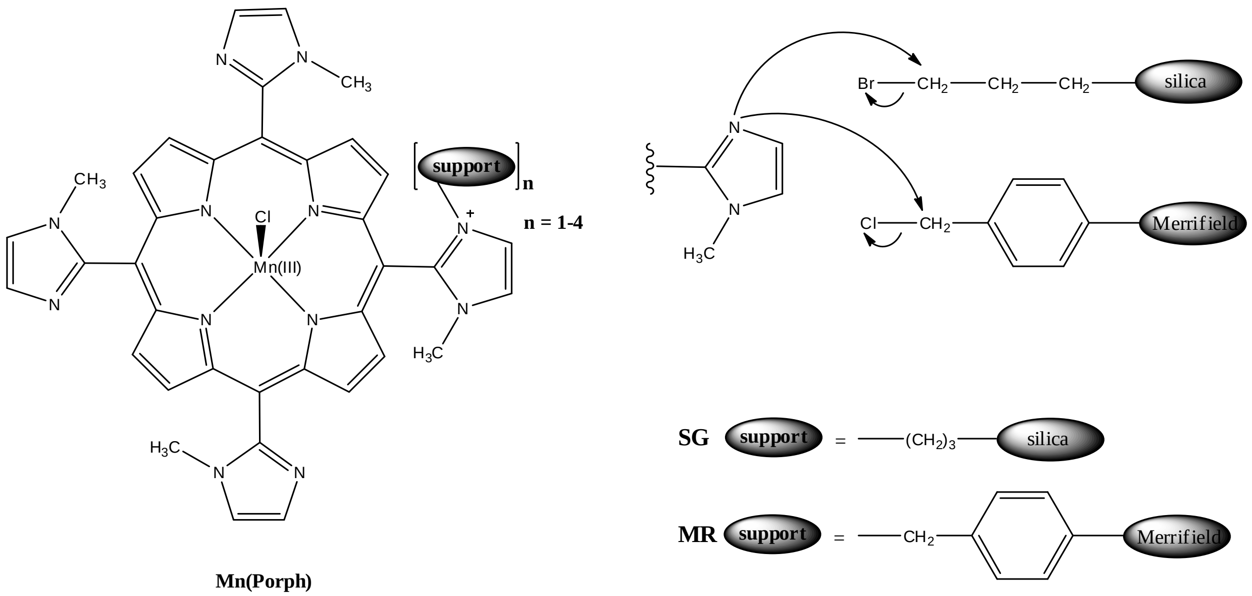

Figure 1. Structure of the immobilized manganese porphyrin (**Mn(Porph))**. The supports are a functionalized silica (3-bromopropylfunctionalized silica gel) and a Merrifield resin (**SG** and **MR,** respectively).

For the Merrifield resin based heterogeneous catalyst [**Mn-(Porph)-MR**], two different conditions were used being the principal difference the temperature of the immobilization. In the first procedure, designed by **MR-Batch-1**, the **MR** was added to a DMF solution of Mn(TMImP)Cl and the reaction was left at 80 ºC under strong stirring for 2 days in an inert atmosphere (N_2), plus 24 hours at r.t. before filtration. Under these conditions, the experimental loading obtained was 0.75% far from the maximum expected one, 4.78% (w/w) if all the metalloporphyrin added was incorporated into the solid. In the second procedure (**MR-Batch-2**), aiming to improve the load of catalyst, the ratio catalyst/**MR** was slightly increased to 6.6% (w/w) and the immobilization was performed at 150 ºC. After 4 hours under N_2, a control showed that almost no free porphyrin was present, and the reaction was terminated as in the previous procedure. Under these conditions the porphyrin loading was really improved to 4.8%. **MR-Batch 3** with the same loading of 4.8 % was obtained under similar conditions of **MR-Batch-2** which confirmed the reproducibility of the immobilization conditions.

The immobilization in the 3-bromopropylfunctionalized silica gel (**SG**) was also performed in DMF at 150 ºC for 4 hours under N_2, and the work-up was exactly the same as for the **MR** heterogeneous materials. For **SG**-materials, the two batches were prepared using two different theoretical porphyrin/support ratios – 5.2 % (w/w) and 3.6% (w/w). Interestingly, the best loading (4.2%, **SG-Batch-2**) was obtained with the more diluted proportion.

The materials obtained have a light brown colour due to the presence of the metalloporphyrin. Several spectroscopic techniques were used to characterize the new compounds. All the results seem to indicate that the porphyrin was incorporated into the new material. For the immobilized systems, diffuse reflectance (Figure 2-A), FT-IR (Figure 2-B) and SEM (Figure 3) were used to characterize the materials. The diffuse reflectance spectra show the usual electronic profile for this kind of materials (Figure 2A). The visible spectra in solution of the **Mn(Porph)** is characterized by a strong Soret band at about 455–465 nm and one Q-band between 550 and 650 nm (Figure 2A). The diffuse reflectance spectra of these materials were similar, showing the Q-band observed in solution spectra but with the relative intensity of the Soret band comparatively diminished, as it is possible to observe in the case of **Mn(Porph)-SG** (Figure 2A). In the case of **Mn(Porph)-MR** the Soret band is not seen in the spectra, however this is a characteristic of some porphyrins, probably due to the very dark material or to some aggregation. In the same figure, the UV-Vis spectra of the **Mn(Porph)** in CH_3CN solution, of the **Mn(Porph)** powder and of the supports (**MR** and **SG**) are also shown for comparison.

The infrared spectra are shown in Figure 2B, where it can be seen the spectra of **MR**, **Mn(Porph)-MR**, **Mn(Porph)** and its charged complex (the cationic manganese porphyrin, a N-methylated catalyst). Unfortunately, the infrared spectra for **Mn(Porph)-SG** was not useful, due to the O-H stretch band of silica, which overlaps the other bands.

Scanning electronic microscopy (SEM) images were taken before (A) and after (B-I) incorporation of the metalloporphyrin (Figure 3), showing some differences on the materials surface. All the characterization results indicate that the metalloporphyrin used is present in the solid compounds obtained without noticeable changes.

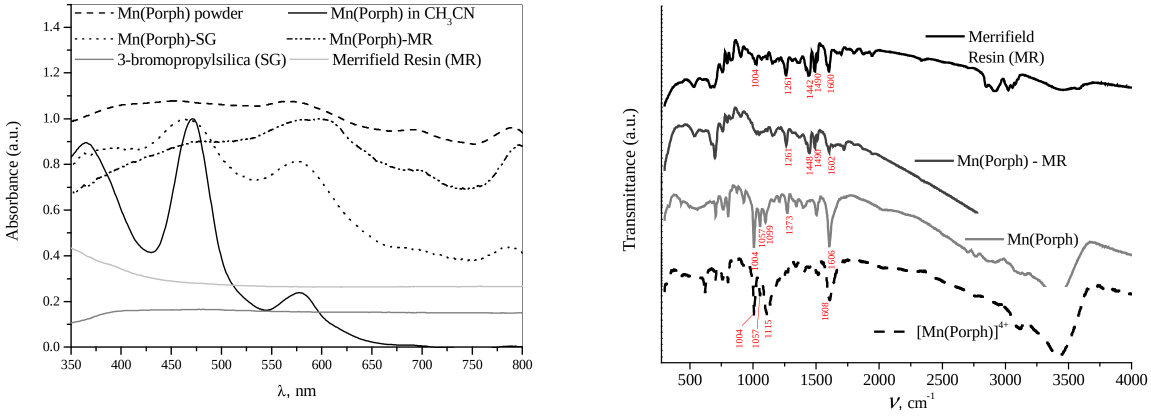

(A) (B)

Figure 2. (A) Electronic profile for the Merrifield resin (**MR**), the 3-bromopropylsilica (**SG**), the Mn(Porph) powder, the immobilized materials (diffuse reflectance) and the metalloporphyrin in CH_3CN solution (UV-Vis); (B) FT-IR for Merrifield resin (**MR**), **Mn(Porph)-MR**, **Mn(Porph)** and $[Mn(Porph)]^{4+}$ (*N*-methylated **Mn(Porph)**).

Scheme 1. Routes for the preparation of the heterogeneous catalysts; 3-bromopropylfunctionalized silica gel (SG); Merrifield resin (MR).

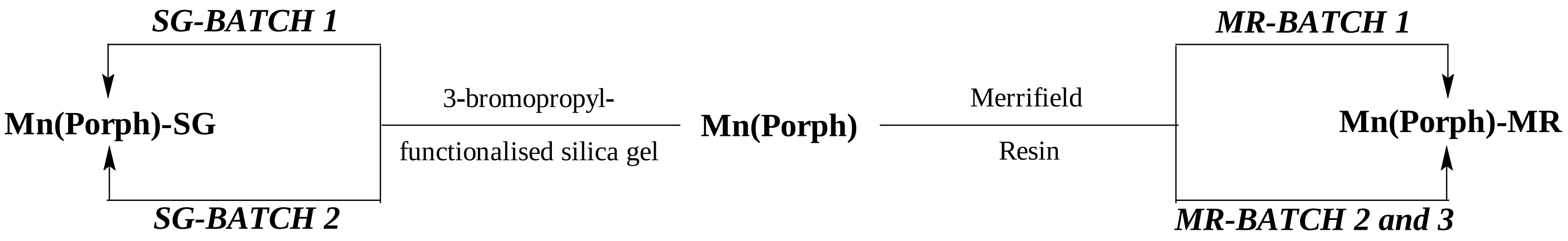

BATCH 1: 16.5 mg ($2.29\text{x}10^{-5}$ mol) of **Mn(Porph)**, 295.5 mg of **SG**, 153 ºC, DMF, $N_{2(g)}$, 4 hours.

BATCH 2: 15,1 mg ($2,10\text{x}10^{-5}$ mol) of **Mn(Porph)**, 405.5 mg of **SG**, 153 ºC, DMF, $N_{2(g)}$, 4 hours.

BATCH 1: (1) 25.2 mg ($3.50\text{x}10^{-5}$ mol) of **Mn(Porph)**, 502.6 mg of **MR**, 80 ºC, DMF, $N_{2(g)}$, 48 hours; (2) 24 hours under stirring.

BATCH 2: 39.7 mg ($5.52\text{x}10^{-5}$ mol) of **Mn(Porph)**, 563.1 mg of **MR** 150 ºC, DMF, $N_{2(g)}$, 4 hours. (BATCH 2)

BATCH 3: 16.3 mg ($2.27\text{x}10^{-5}$ mol) of **Mn(Porph)**, 227.8 mg of **MR** 150 ºC, DMF, $N_{2(g)}$, 4 hours. (BATCH 3)

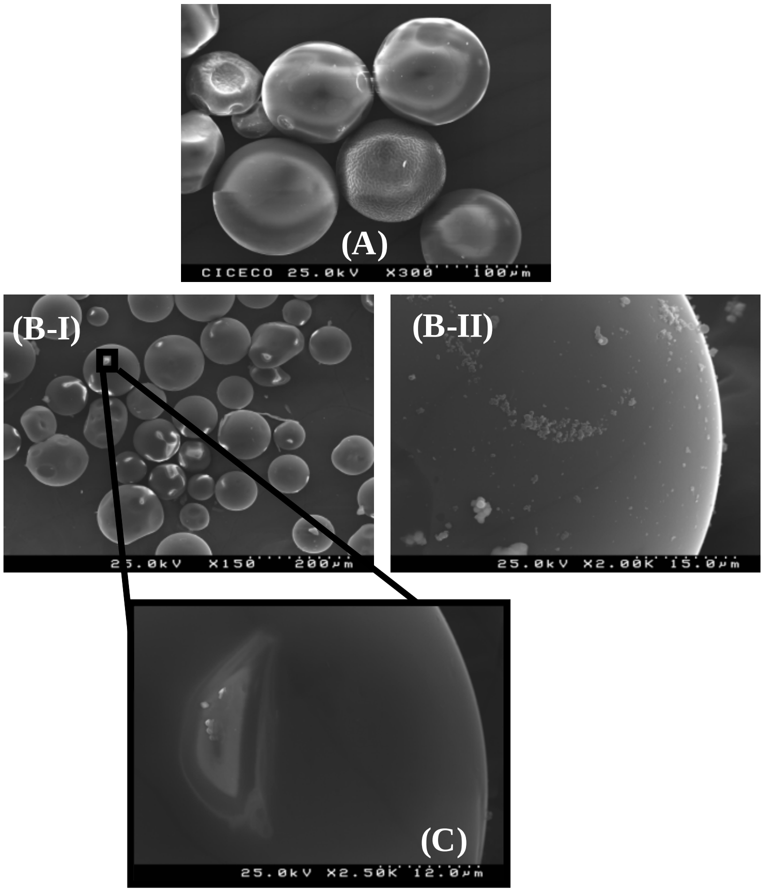

Figure 3. SEM images taken from: **(A)** MR; **(B-I) Mn(Porph)-MR** (Batch 3) before and **(B-II)** after the catalytic reaction; **(C)** a zoom on **(B-I)** image.

2.2. Catalytic activity for *cis*-cyclooctene epoxidation reactions

To assess the catalytic properties of the new heterogeneous materials, the oxidation of *cis*-cyclooctene was carried out using H_2O_2 and *t*-BuOOH as the oxidants. In Table 1 are summarized the results obtained with the different **Mn(Porph)-SG** batches and in Table 2 the ones obtained with the **Mn(Porph)-MR** batches. In general the **Mn(Porph)-MR** systems shows higher activity than **Mn(Porph)-SG** counterpart. Although silica containing materials are frequently used as supports in catalysis, some reports highlight the efficiency of **MR** in biomimetic oxidation with metalloporphyrins.[44]

Regarding the catalytic activity and recyclability registered with the **Mn(Porph)-SG** systems the results summarized in Table 1 show that the high conversion observed in the first cycle suffers a drastic drop with the reuse, independently of the oxidant used, H_2O_2 or *t*-BuOOH.

The results obtained for **Mn(Porph)-SG** allow us to conclude that after the addition of 5-6 equivalents of H_2O_2, the batch 2 (4.19 % loading) material gives rise to a higher conversion in the first (99.2 %) and in the second cycles (52.7 %), against 79.4 % and 2.2 %, respectively, for batch 1 (1.08 % loading). This can be related to the amount of **Mn(Porph)** anchored into the silica materials, since batch 2 presents a nearly 4 times higher loading than batch 1. Unfortunately, the efficiency of batch 2 in the presence of H_2O_2 drops drastically in the third cycle (entry 7). It is worth to refer that the reactions were stopped when, after two successive oxidant additions, the substrate conversion remained constant (see experimental section). Moreover, under homogeneous conditions, the same **Mn(Porph)** gives rise to 100 % of conversion after 75-90 min and 2.5-3.0 equivalents of H_2O_2, under similar reaction conditions, so the somewhat longer reaction times are not surprising under heterogeneous conditions.

Table 1. Experimental results obtained for *cis*-cyclooctene oxidation catalyzed by heterogeneous catalysts **Mn(Porph)-SG** with *t*-BuOOH or H_2O_2.(a)

Entry	Batch	Oxidant	Oxidant addition frequency (min)	Oxidant (equiv.)	Time of reaction (min)	Conversion(b) (%)	Cycles
1	Batch 1	*t*-BuOOH	30	6	360	81.2	1
2	Batch 1	*t*-BuOOH	30	6	360	12.8	2
3	Batch 1	H_2O_2	30	6	360	79.4	1
4	Batch 1	H_2O_2	30	5	300	2.2	2
5	Batch 2	H_2O_2	15	5	150	99.2	1
6	Batch 2	H_2O_2	15	6	180	52.7	2
7	Batch 2	H_2O_2	15	3	90	4.9	3
8(c)	---	H_2O_2	15	6	180	0	---

(a)substrate (0.3 mmol), catalyst (50 mg) and co-catalyst (3.3 mmol). Each oxidant addition corresponds to a half of the initial substrate concentration (*i.e.*, 0.15 mmol). All reactions were carried out in CH_3CN (0.5 mL); (b)the corresponding epoxide was obtained as the only product; (c)blank reaction, using just the support with co-catalyst (acetic acid).

Table 2. Experimental results obtained for *cis*-cyclooctene oxidation catalyzed by heterogeneous catalysts **Mn(Porph)-MR** with *t*-BuOOH or H_2O_2.(a)

Entry	Batch	Oxidant	Oxidant addition frequency (min)	Oxidant (equiv.)	Time of reaction (min)	Conversion(b) (%)	Cycles
1	Batch 1	*t*-BuOOH	30	6	360	89.5	1
2	Batch 1	*t*-BuOOH	30	6	360	53.2	2
3	Batch 1	*t*-BuOOH	15	3.5	210	70.4	1
4	Batch 1	*t*-BuOOH	15	3.5	210	60.0	2
5	Batch 1	H_2O_2	30	6	360	96.7	1
6	Batch 1	H_2O_2	30	6	360	57.0	2
7	Batch 2	H_2O_2	15	5	150	100	1
8	Batch 2	H_2O_2	15	6	180	96.4	2
9	Batch 2	H_2O_2	15	6	180	91.4	3
10	Batch 2	H_2O_2	15	6	180	68.7	4
11	Batch 3	H_2O_2	15	5	150	100	1
12	Batch 3	H_2O_2	15	6	180	100	2
13	Batch 3	H_2O_2	15	6	180	85.8	3
14(c)	---	H_2O_2	15	6	180	0	---

(a)substrate (0.3 mmol), catalyst (50 mg) and co-catalyst (3.3 mmol). Each oxidant addition corresponds to a half of the initial substrate concentration (*i.e.*, 0.15 mmol). All reactions were carried out in CH_3CN (0.5 mL); (b)the corresponding epoxide was obtained as the only product; (c)blank reaction, using just the support with co-catalyst (acetic acid).

The first experiments performed with **Mn(Porph)-MR** batch 1 (Table 2) in the presence of H_2O_2 (entries 5,6) and *t*-BuOOH (entries 1-4) show that the best conversion in the first cycle was obtained with the first oxygen donor (96.7% *vs* 89.5%). However, in both cases the conversions obtained drop significantly to *ca.* 50% with the catalyst recycle (entries 2,6). With this batch no improvement on the recycle was observed when the addition of the oxidant was performed at each 15 min instead of 30 min (entries 3,4 for *t*-BuOOH; data not shown for H_2O_2). The differences in the procedures employed in the synthesis of the heterogeneous catalysts and consequently in the amount of porphyrin immobilized are reflected in the catalytic efficiency observed during the epoxidation reactions with **Mn(Porph)-MR** batches 2 and 3.

The results obtained for **Mn(Porph)-MR** after the addition of 5-6 equivalents of H_2O_2 are always higher than those registered for **Mn(Porph)-SG**. Conversions between 96.7-100% were obtained in the first cycle, the **Mn(Porph)** catalyst loading representing the major factor of differentiation. Batch 1 (0.75% loading) gives only 57.0% of conversion in the second cycle, whereas batches 2 (4.83% loading) and 3 (4.80% loading) give rise to 96.4 and 100%, respectively. So, **Mn(Porph)-MR** batch 2 exhibits high catalytic efficiency, that is maintained after being recycled three times; even in the fourth recycle an agreeable conversion of near 70% was attained (entries 7-10). To ascertain if the reproducibility of that feature is not related specially with batch 2, the oxidation experiments were repeated with **Mn(Porph)-MR** batch 3 with the same metalloporphyrin content. As expected, the efficiency of the system is maintained when the **Mn(Porph)-MR** batch 3 was used as catalyst (entries 11-13). These results show that, under the same conditions, **Mn(Porph)-SG** presents lower performance when compared with the **Mn(Porph)-MR** materials. These can be attributed to a higher stability of the covalent linkage established between the **Mn(Porph)** and the **MR** support, since several cycles are viable for the **Mn(Porph)-MR** material, and no catalyst leaching seems to occur, as can be seen on Figure 4.

The control experiments (entries 8 in table 1 and 14 in table 2) confirm that, in the absence of the Mn-porphyrin, no conversion is observed, even using acetic acid (the co-catalyst) in the reaction medium. Hence, the possibility of forming peroxyacetic acid *in situ* as the putative epoxidation reagent can be disregarded.

Using the conditions described in entry 7 (Table 2), additional experiments were run to evaluate the possibility of bleaching during catalysis reactions. Figure 4 illustrates the bleaching and the recycling assays. Apparently, the decrease in catalytic activity observed from the first to the fourth cycles using **Mn(Porph)-MR** (Figure 4) was not due to the bleaching of the catalyst. Thus, a possible explanation can be attributed to the degradation or the inactivation of the catalyst, along the catalytic cycles. Scanning electronic microscopy (SEM) images were taken before and after the first cycle (Figure 3 B-I and 3 B-II), showing some differences on the materials surface, which can be the reason for the registered decrease in the catalytic activity.

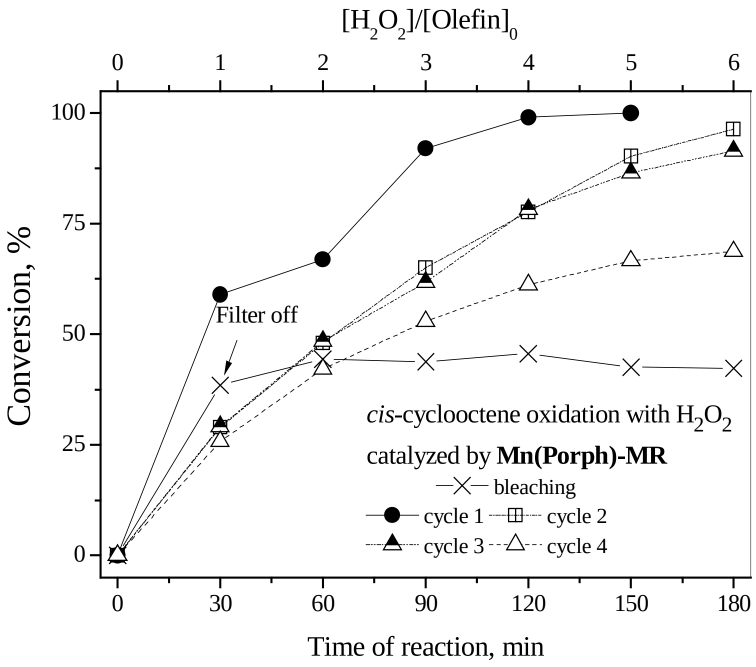

Figure 4. Catalyst recycling and bleaching experiments with **Mn(Porph)-MR** for *cis*-cyclooctene oxidation with H_2O_2. The results shown for cycles 1-4 are related to entries 7-10 (Table 2).

2.3. Styrene, cyclohexene and geraniol oxidation

Additional reactions were performed to check the catalytic efficiency of the best material **Mn(Porph)-MR** towards other olefins such as styrene, cyclohexene and geraniol. The results obtained in those studies are summarized in Tables 3-5.

It is known that styrene epoxidation is not a clean reaction, since side-products like phenylacetaldehyde and benzaldehyde can be observed in biomimetic oxidations catalyzed by metalloporphyrins[45,46] and cytochrome P450 enzymes.[47] In this work, high substrate conversion was registered for the first four cycles, decreasing in the 5th cycle, while high selectivity to the styrene epoxide (*ca* 90%) was observed up to 5 cycles (Table 3, entries 1-5). The selectivity for the phenylacetaldehyde (7%) and benzaldehyde (3%) was not altered during the recycles. Under homogeneous conditions, the tetracationic metalloporphyrin gives the same products, although the selectivity for the epoxide can be improved by decreasing the substrate/catalyst ratio (Table 3, entries 6,7).

Regarding cyclohexene oxidation, the high conversion (97-100%) accompanied by high selectivity for the cyclohexene oxide (*ca* 90%) were kept almost constant in all the catalyst recycles. The selectivity for cyclohex-2-en-1-ol and cyclohex-2-en-1-one, resulting from allylic oxidation (global yield ~9%) did not suffer also great fluctuations during the catalyst reuse (Table 4, entries 1-4), although the selectivity is higher than that observed under homogeneous conditions (Table 4, entries 5,6). As it was already mentioned, for this olefin, the efficiency was kept almost constant in all the catalyst recycles, while in homogeneous conditions the catalyst stability was lower than 50% at the end of the reaction (from UV/Vis spectrum; not shown). It is known that cyclohexene auto-oxidation can involve molecular oxygen participation through a radical pathway,[48] thus more than a single active catalytic species being present.[49]

As expected, the 6,7-epoxide was the main product obtained for geraniol oxidation, followed by the 2,3-epoxide isomer and the corresponding 2,3,6,7-diepoxide (Table 5, entries 1-4). Homogeneous conditions yielded a slightly higher selectivity for 6,7-epoxide than the heterogeneous conditions (Table 5, entry 5). Curiously, under heterogeneous conditions a little bit more 2,3-epoxide was obtained, a typical situation found in reactions where the metal centre undergoes attraction to the hydroxyl group present in the geraniol structure.[50] Such an observation indicates that, under some circumstances, the somewhat analogous protein matrix microenvironment created by the support - in heme enzymes this is the role of the protein matrix which surrounds the prosthetic group - can drive some changes on the selectivity of the reaction.[51] The efficiency observed with this kind of metalloporphyrins can be due to some structural features which do both effects, the electron withdrawing effect and the protection of the porphyrin ring. The conversion obtained in the first cycle (*ca* 70%), after a fall in the second run into ~50%, maintain this last value almost constant in the posterior reuses.

Table 3. Styrene oxidation with H_2O_2 catalyzed by **Mn(Porph)-MR** following the conditions described in Table 2 (for batch 3, entry 11).[(a)] In the homogeneous conditions the **Mn(Porph)** used was [Mn(TDMImP)Cl]I_4 (cationic metalloporphyrin).

Entry	**Olefin**	**Cycle**	**Selectivity (%)**			**Conversion (%)**	**Time of reaction (min)**
			Styrene oxide	**Phenylacetaldehyde**	**Benzaldehyde**		
1	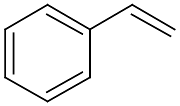 Styrene	1	90.9 ± 2.1	7.2 ± 3.0	2.3 ± 0.4	92.1	180
2		2	90.6 ± 1.4	7.4 ± 2.2	2.4 ± 0.3	89.8	180
3		3	88.6 ± 2.3	6.9 ± 1.8	4.5 ± 0.8	84.4	180
4		4	89.4 ± 5.8	7.7 ± 4.6	2.9 ± 1.5	78.8	180
5		5	88.1 ± 1.7	6.6 ± 2.5	5.3 ± 0.8	57.9	180
		Olefin/Catalyst ratio – homogeneous[(b)]					
6[(c)]		75	> 95	traces	traces	100	60
7[(d)]		300	81	18	< 1	57	60

[(a)] reaction conditions (batch 3, Table 2, entry 11): substrate/catalyst/co-catalyst = 0.3 mmol/0.522 μmol/3.325 mmol; CH_3CN, 0.5 mL. Each oxidant addition corresponds to a half of the initial substrate concentration (*i.e.*, 0.15 mmol). [(b)] homogeneous conditions: solvent: acetonitrile (2 mL of total volume); concentration of the catalyst employed was 2.5×10^{-4} mol.dm^{-3}; co-catalyst: acetic acid (0.42 mmol); the oxidant used was 30% (w/w) aqueous H_2O_2 diluted in acetonitrile (1:10) and its addition was made gradually each 15 min of reaction. Each H_2O_2 addition corresponds to a half-substrate amount; [(c)] from reference [24]. [(d)] similar to reference [24], except for the Olefin/Catalyst ratio.

Table 4. Cyclohexene oxidation with H_2O_2 catalyzed by **Mn(Porph)-MR** following the conditions described in Table 2 (for batch 3, entry 11).(a) In the homogeneous conditions the **Mn(Porph)** used was [Mn(TDMImP)Cl]I_4 (cationic metalloporphyrin).

Entry	**Olefin**	**Cycle**	**Selectivity (%)**			**Conversion (%)**	**Time of reaction (min)**
			Cyclohexene oxide	**Cyclohex-2-en-1-ol**	**Cyclohex-2-en-1-one**		
1	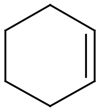 Cyclohexene	1	90.8 ± 1.9	3.9 ± 2.4	5.4 ± 3.7	100	150
2		2	90.7 ± 2.5	3.3 ± 2.1	5.9 ± 3.7	98.9	150
3		3	91.0 ± 2.0	3.4 ± 2.2	5.6 ± 3.7	98.5	150
4		4	91.3 ± 2.0	3.5 ± 2.3	5.2 ± 3.7	97.4	150
		Olefin/Catalyst ratio – homogeneous(b)					
5(c)		75	100	0	0	100	60
6(d)		300	95	3	2	57	60

(a)reaction conditions (batch 3, Table 2, entry 11): substrate/catalyst/co-catalyst = 0.3 mmol/0.522 µmol/3.325 mmol; CH_3CN, 0.5 mL Each oxidant addition corresponds to a half of the initial substrate concentration (*i.e.*, 0.15 mmol). (b)homogeneous conditions: solvent: acetonitrile (2 mL of total volume); concentration of the catalyst employed was 2.5 x 10^{-4} mol.dm^{-3}; co-catalyst: acetic acid (0.42 mmol); the oxidant used was 30% (w/w) aqueous H_2O_2 diluted in acetonitrile (1:10) and its addition was made gradually each 15 min of reaction. Each H_2O_2 addition corresponds to a half-substrate amount; (c)from reference [24]. (d)similar to reference [24], except for the Olefin/Catalyst ratio.

Table 5. Geraniol oxidation with H_2O_2 catalyzed by **Mn(Porph)-MR** following the conditions described in Table 2 (for batch 3, entry 11).[(a)] In the homogeneous conditions the **Mn(Porph)** used was $[Mn(TDMImP)Cl]I_4$ (cationic metalloporphyrin).

Entry	**Olefin**	**Cycle**	**Selectivity (%)**			**Conversion (%)**	**Time of reaction (min)**
			2,3-epoxy geraniol	**6,7-epoxy geraniol**	**2,3,6,7-diepoxy geraniol**		
1	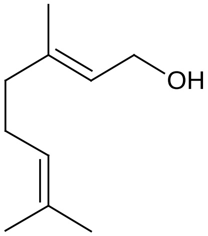 Geraniol	1	36.2 ± 1.8	49.2 ± 1.9	14.6 ± 3.2	72.7	180
2		2	41.2 ± 1.0	48.9 ± 1.7	9.9 ± 2.6	53.4	180
3		3	39.8 ± 1.1	50.5 ± 1.1	9.7 ± 2.1	54.0	180
4		4	39.3 ± 4.7	46.5 ± 1.6	14.2 ± 5.6	51.2	180
		Olefin/Catalyst ratio – homogeneous					
5[(b)]		300	30	58	12	67	60

[(a)] reaction conditions (batch 3, Table 2, entry 11): substrate/catalyst/co-catalyst = 0.3 mmol/0.522 μmol/3.325 mmol; CH_3CN, 0.5 mL Each oxidant addition corresponds to a half of the initial substrate concentration (*i.e.*, 0.15 mmol). [(b)] from reference [52].

2.4. Efficiency rationale

It is know that the manganese(III) complexes of 5,10,15,20-tetrakis(2,6-dichlorophenyl)porphyrin [Mn(TDCPP)Cl] and 5,10,15,20-tetrakis(pentafluorophenyl) porphyrin [Mn(TPFPP)Cl] are two of the most important compounds in porphyrins' catalytic biomimetic oxidation. Their efficiency is related to the strong electron-withdrawing character and the protection effect. Figure 5 illustrates the putative structural similarities among [Mn(TDCPP)Cl], [Mn(TPFPP)Cl], [Mn(4-TDMImP)Cl]$^{4+}$ as well as the immobilized analogue of the latter, where the highlights show the bulky substituents near the macrocycle.

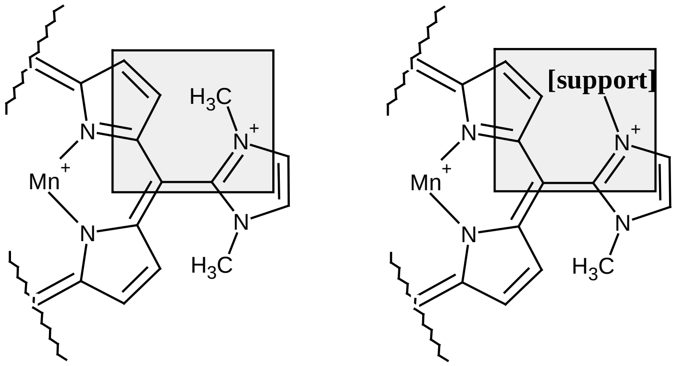

[Mn^{III}(4-TDMImP)Cl]$^{4+}$ **[Mn^{III}(4-TDMImP)Cl]$^{4+}$——[support]**

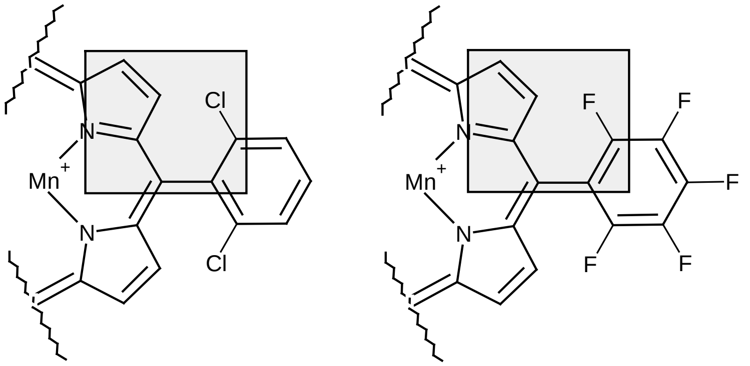

Mn^{III}(TDCPP)Cl **Mn^{III}(TPFPP)Cl**

Figure 5. Structural similarities amongst some manganese (III) porphyrin derivatives. The highlight shows the bulky substituents near the macrocycle.

One way to assess the robustness of metalloporphyrins is reached by comparing the UV/Visible spectrum in neutral and in acidic media (*e.g.*, with and without hydrochloric acid).[53] The differences observed point out the orbital cross susceptibility, which is due to the substituent effect. From the practical point of view, such spectral differences are given by intensity, profile and number of Q-bands (mainly Q_x (0,0)).

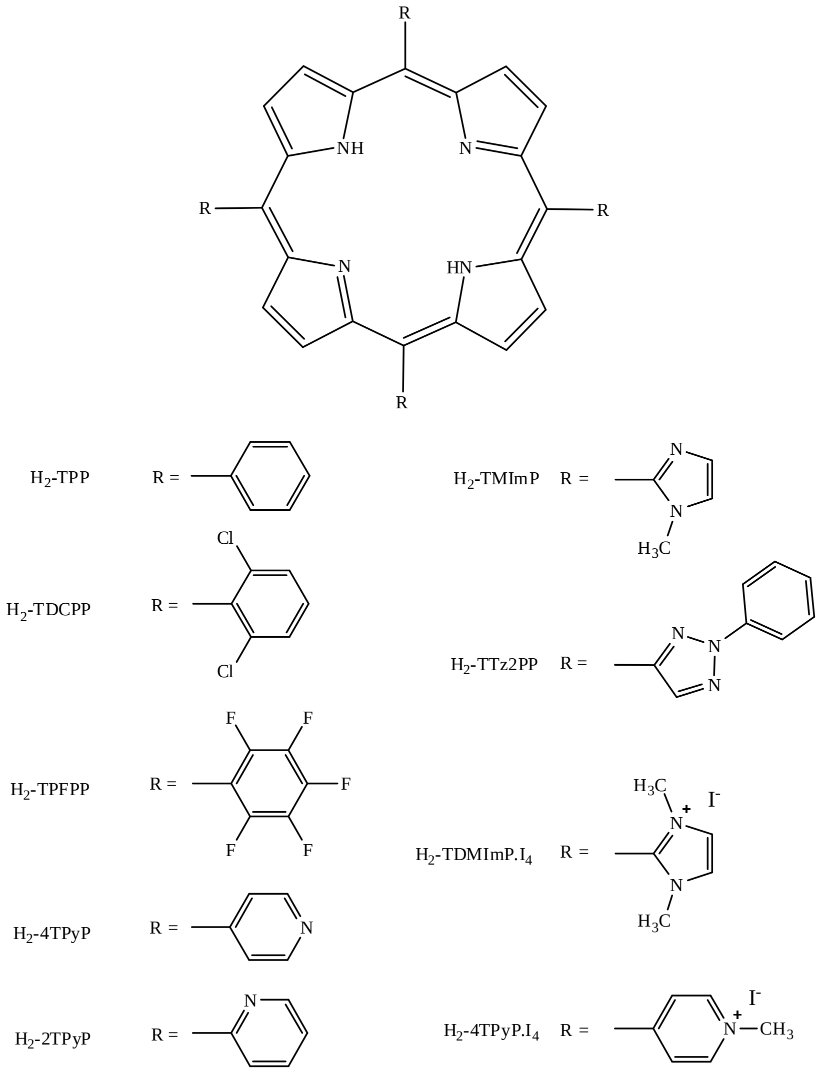

Figure 6. Structures and acronyms of the porphyrin derivatives studied

The results summarized in Table 6 (please refer to Figure 6 for the structures and acronyms of the porphyrin derivatives) indicate that electron-withdrawing groups attached to the porphyrin ring turn the metallic center highly electrophilic. Nonetheless, ionic substituents avoid the reaction once they change the oxidation state of manganese hindering the oxygen atom transfer from the active porphyrin species to the substrate.

The results show that H_2-TPP was stabilized in acidic media, once its conjugated acid $[H_4\text{-TPP}]^{2+}$ exhibited a batochromic shift ($\Delta\lambda$= +16 nm), thus indicating an extension in conjugation between the phenyl rings and the macrocycle (entries 1,2).

On the other hand, the phenyl derivatives H_2-TDCPP (entries 3,4) and H_2-TPFPP (entries 5,6), which are precursors of high stable and efficient catalysts, originated hypsochromic shifts indicating that the substituents exhibit a strong electron-withdrawing effect on the macrocycle and, due to steric effects, no conjugation can be thought. Dealing with porphyrins bearing heterocyclic units in the *meso*-positions (entries 7-18), entries 7-8 show the pair H_2-4TPyP/$[H_4\text{-4TPyP}]^{2+}$ and entries 9,10 show the isomeric pair H_2-2TPyP/$[H_4\text{-2TPyP}]^{2+}$. By comparing the results obtained for these systems, it can be seen that in the first case a stabilization gave a shift of $\Delta\lambda$= +24 nm, whereas in the latter case the shift was $\Delta\lambda$= +17 nm, indicating that steric hindering is the limiting feature to explain such differences. In the same way, when the analysis is carried out to H_2-TMImP (entry 11), the hindering effect due to a methyl group attached to one imidazolyl nitrogen is responsible by a shift of +6 nm (entry 12). The behavior observed among H_2-4TPyP, H_2-2TPyP and H_2-TMImP reflects the differences in steric and electronic properties due to the *meso*-substituent. The imidazolyl group is more electronegative than the pyridil moiety. But such difference has no correlation with the ring size, since a great stabilization was observed with the derivative H_2-TTz2PP (entries 13,14 for ionic species), which has a triazolyl group attached to the porphyrin ring. The most interesting results were observed when the analyses were carried out with the tetracationic derivatives H_2-TDMImP.I_4 and H_2-4TMPyP.I_4. The first correlation to be assigned is the difference between cationic and its neutral counterpart for each derivative. In the case of H_2-4TMPyP.I_4, a slight shift of +2 nm (entry 18) was observed which is completely different when comparing with the neutral parental porphyrin profile (entry 8). Also the spectrum of compound H_2-4TMPyP.I_4 is quite different from that of the same compound in neutral system (aqueous media; Figure 7). In the case of H_2-TDMImP.I_4, no changes were observed in the electronic spectrum in acidic media (Figure 7). Such feature indicates that the inner hydrogens resist to protonation even with concentrated HCl, thus suggesting that imidazolium groups are strong electron-withdrawing substituents. The introduction of another methyl group to the imidazolyl substituent enhances the electron-withdrawing effect as well as the bulkiness, thus turning difficult the conjugation with the macrocycle. These observations are intimately related with orbital stabilization (Figure 8). Regarding the structural aspects, there is a similarity between H_2-2TPyP and H_2-TMImP. These similarities will be also observed in their cationic forms and in the metallocomplexes. In this way, some theoretical hypothesis established for the first derivative can be applied, at a given extension, to the latter compound. Jin and Groves[54] studied the reactivity profile between the regioisomers $[H_2\text{-4TMPyP}]^{4+}$ and $[H_2\text{-2TMPyP}]^{4+}$ and attributed the differences to the orbital stabilization. The cationic derivative $[H_2\text{-2TMPyP}]^{4+}$ resists to protonation even at pH=0,[54] such as observed for the $[H_2\text{-TDImP}]^{4+}$. This uncommon feature decreases the donation character of A_2u molecular orbital, which undergoes the influences of *meso*-substituent groups (as can be seen in Figure 8) and increases the gap energy between A_2u-e_g molecular orbitals, justifying the reported behavior. In the metallocomplex form (*e.g.*, manganese complex), the same behavior is expected to take place.

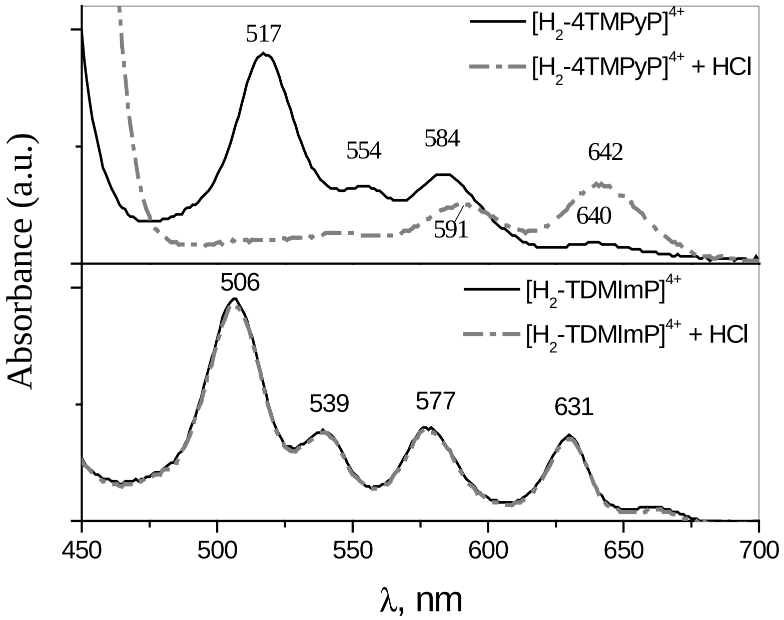

Figure 7. Electronic spectra of tetracationic derivatives $[H_2\text{-4TMPyP}]^{4+}$ and $[H_2\text{-TDMImP}]^{4+}$ with and without concentrated HCl.

Table 6. Electronic parameters of the Q-bands in metalloporphyrins. Intensities and wavelengths recorded in neutral and in acidic media.

Entry	Derivative	Solvent	Qy (0;1)	Qy (0;0)	Qx (0;1)	Qx (0;0)	Δλ, nm	
							Qy	Qx
1	H_2-TPP	$CHCl_3$	514	549	588	644		
2	$[H_4\text{-TPP}]^{2+}$	$CHCl_3$ + HCl conc.		608		660	+59	+16
3	H_2-TDCPP	$CHCl_3$	512	539*(sh.)*	587	657		
4	$[H_4\text{-TDCPP}]^{2+}$	$CHCl_3$ + HCl conc.		588		637	+49	-20
5	H_2-TPFPP	$CHCl_3$	505	534*(sh.)*	582	656		
6	$[H_4\text{-TPFPP}]^{2+}$	$CHCl_3$ + HCl conc.		589		641	+55	-15
7	H_2-4TPyP (a)	$CHCl_3/CH_3OH$ (85:15)	511	545	585	642		
8	$[H_4\text{-4TPyP}]^{2+}$	$CHCl_3/CH_3OH$ (85:15) + HCl conc.		616		666	+31	+24
9	H_2-2TPyP (a)	$CHCl_3/CH_3OH$ (85:15)	510	542	586	647		
10	$[H_4\text{-2TPyP}]^{2+}$	$CHCl_3/CH_3OH$ (85:15) + HCl conc.		612		664	+70	+17
11	H_2-TMImP (a)	$CHCl_3$	512	546*(sh.)*	585	657		
12	$[H_4\text{-TMImP}]^{2+}$	$CHCl_3$ + HCl conc.		607		663	+22	+ 6
13	H_2-TTz2PP (a)	$CHCl_3$	519	555	593	656		
14	$[H_4\text{-TTz2PP}]^{2+}$	$CHCl_3$ + HCl conc.		624*(sh.)*		677	+69	+21
15	$H_2\text{-TDMImP.I}_4$	H_2O	506	539	577	631		
16	$[H_4\text{-TMImP.I}_4]^{2+}$ (b)	H_2O + HCl conc.	~ 506 (c)	539	~ 577 (c)	630	0	-1
17	$H_2\text{-4TMPyP.I}_4$	H_2O	517	554	584	640		
18	$[H_2\text{-4TMPyP.I}_4]^{2+}$ (b)	H_2O + HCl conc.		591		642	+37	+2

(a)protonation of substituents was disregarded; (b)counter-ion charge was considered; (c)no change was recorded.

Those observations made for $[H_2\text{-TDMImP}]^{4+}$ play an important role to explain the high catalytic efficiency observed in oxidation reactions using the immobilized systems. A different efficiency for the system **Mn(Porph)-SG** should be expected; a probable explanation must be entirely structural, since the linear propyl moiety that links the porphyrin to the support (silica gel) does not confer protection against oxidative degradation, while the tolyl group linking the porphyrin to the **MR** support is bulkier and protects better the macrocycle from oxidative attack.

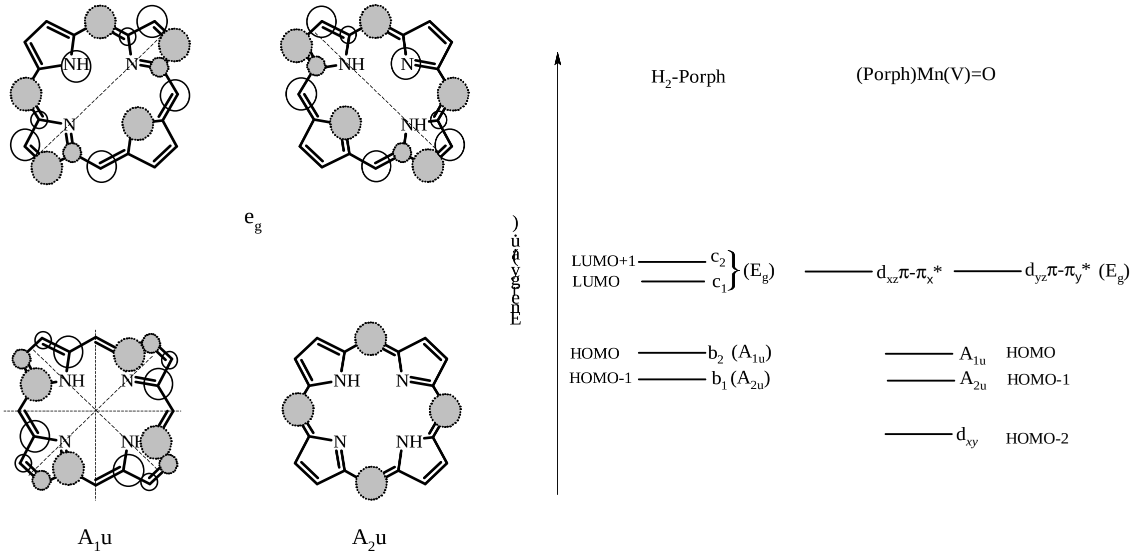

Figure 8. Molecular orbital distribution according to Martin Gouterman theory for H_2-Porph (left)[53,54] and orbital distribution according to DeAngelis and Groves[55] proposal for elusive species (2-TMPyP)Mn(V)=O (right). The diagram does not account the energy differences amongst orbitals.

3. CONCLUSIONS

This work presents a new heterogeneous catalytic system based on an imidazolyl manganese porphyrin, able to selectively oxidize olefins exclusively or mainly to their corresponding epoxides. The catalytic efficiency seems to be influenced by the synthetic conditions used during the immobilization reactions. The silica support did not yield a totally satisfactory heterogeneous oxidation system, even if *t*-BuOOH in decane is used as the oxygen donor, thus avoiding the water present in aqueous hydrogen peroxide. The conditions studied allow high reaction performance using an environmentally benign oxidant (H_2O_2), the catalyst being recycled up to four times without appreciable loss in efficiency. The efficiency observed can be explained by molecular orbital stabilization achieved by the linkage between the metallocomplex and the support. The lower catalytic efficiency observed for **Mn(Porph)-SG** in comparison with **Mn(Porph)-MR** may be attributed to structural differences, owing to the support linker.

4. EXPERIMENTAL

All solvents and reagents were used as received without further purification, except for pyrrole, which was distilled before use. Pyrrole, *cis*-cyclooctene, styrene, geraniol, cyclohexene, *n*-octane, *tert*-butylhydroperoxide (*t*-BuOOH), 3-bromopropyl functionalized silica gel (200-400 mesh, 1.5 mmol/g), Merrifield resin (30-40 mesh, 2.0 mmol/g, 1% cross-linked) and dimethylformamide were purchased from Aldrich. Propionic acid and acetonitrile were obtained from Merck whereas aqueous hydrogen peroxide (30% w/w) was obtained from Riedel-de-Häen. Acetic acid was purchased from PanReac. The Membrane filter N16 (0.2 μm; ϕ = 50 mm) was used to filter the crude reaction in order to separate the heterogenized materials during catalyst synthesis.

GC-FID analyses were performed using a Varian 3900 chromatograph, whereas GC–MS analyses were performed using a Finnigan Trace GC-MS (Thermo Quest CE instruments) both using helium as the carrier gas (35 cm/s) and equipped with a fused silica capillary 5% phenyl 95% dimethylpolysiloxane column (30 m x 0.25 mm i.d.; 25 μm film thickness).

The ^1H NMR spectra were recorded in a Bruker Avance 300 at 300.13 MHz. $CDCl_3$ was used as solvent and TMS as the internal reference; chemical shifts are expressed in δ (ppm). The mass spectrometry analyses were carried out in a 4800 MALDI TOF/TOF Analyzer, Applied

Biosystems, with and without matrix. The UV/Visible measurements were recorded in a double beam spectrophotometer Shimadzu UV-2501 PC. C, H, N elemental analyses were performed on a Leco CHNS-932 apparatus. Infrared spectra were obtained on a Mattson 7000 spectrophotometer using KBr pellets. Diffuse reflectance spectra were registered on a Jasco V-560 spectrophotometer, using MgO as reference. Scanning electron microscope images (SEM) were recorded on a Hitachi S-4100 microscope.

4.1. Porphyrin and manganese(III) complex syntheses

The free-base porphyrin, 5,10,15,20-tetrakis(1-methylimidazol-2-yl)-21H,23H-porphyrin (H_2-TMImP) was obtained as a mixture of atropoisomers from pyrrole and 1-methylimidazole-2-carboxaldehyde in propionic acid under microwave (MW) irradiation following the method already described by us.[56] The synthesis of the manganese complex was carried out according to procedures described elsewhere.[2,24,52]

Structural characterization was made by ^{1}H NMR spectroscopy and by mass spectrometry (MALDI TOF/TOF) for the free-base porphyrin (H_2-TMImP). The ^{1}H NMR results obtained for the atropoisomers of H_2-TMImP are similar to those already known.[12,24,57]

4.2. Manganese porphyrin immobilization

To immobilize the manganese porphyrin onto the solid supports, a method reported by Tangestaninejad *et al.* was adopted.[36,43] Depending on the support used, some adjustments were done. Scheme 1 shows the procedures adopted in each case and the experimental differences among the batches produced. In a conic flask, and to a DMF solution of the manganese porphyrin, the Merrifield resin (**MR**) or the 3-bromopropyl-functionalized silica gel (**SG**) were added. The mixture was vigorously stirred at a given temperature for a given time (see Scheme 1 for details). After cooling, the material was collected by filtration and thoroughly washed with DMF, methanol, water, ethanol and chloroform, in this order, and dried at 60 ºC overnight. The heterogeneous materials, **Mn(Porph)-MR** or **Mn(Porph)-SG**, were obtained and the load of manganese porphyrin in each material was determined by elemental analysis (from the nitrogen content level). **Mn(Porph)-MR-batch 1**: Porphyrin loading found: 0.75 (calc.: 4.78); **Mn(Porph)-MR-batch 2**: Porphyrin loading found: 4.83 (calc.: 6.59); **Mn(Porph)-MR-batch 3**: Porphyrin loading found: 4.80 (calc.: 6,67); **Mn(Porph)-SG-batch 1**: Porphyrin loading found: 1.08 (calc.: 5.23); **Mn(Porph)-SG-batch 2**: Porphyrin loading found: 4.19 (calc.: 3.59).

4.3. Oxidation procedure

In a typical experiment, based on earlier work by our group,[24,41,42] substrate (0.3 mmol), the catalyst (50.0 mg) and the co-catalyst (acetic acid, 3.325 mmol) were dissolved in acetonitrile (500.0 μL). The mixture was maintained under magnetic stirring at room temperature (25 ± 1 ºC) in the absence of light. Two oxidants were tested in the oxidation reactions: aqueous 30% (w/w) H_2O_2 diluted in acetonitrile (1:10) and *t*-BuOOH (5.0-6.0 M in decane). The oxidant was progressively added in aliquots corresponding to a half-substrate amount (0.15 mmol). The reactions were followed by GC and were stopped when, after two successive oxidant additions, the substrate conversion remained constant or reached 100%.

Finally, the catalyst was recovered by centrifugation, carefully washed with different solvents (acetonitrile, diethyl ether) and dried in an evacuated desiccator overnight before new utilization under similar reaction conditions.

The leaching experiments were made in the same conditions described above but after 30 min of reaction the catalyst was removed by centrifugation and the reaction proceeded for 3 h without the solid.

ACKNOWLEDGEMENTS

The authors would like to thank Fundação para a Ciência e a Tecnologia (FCT, Portugal), the European Union, QREN, FEDER, COMPETE, for funding the Organic Chemistry Research Unit (QOPNA) (PEst-C/QUI/UI0062/2013). Authors also acknowledge the Portuguese National NMR Network (RNRMN), supported with funds from FCT. R. De Paula also thanks FCT for his PhD grant (SFRH/BD/25666/2005).

References

[1] F. Montanari, L. Casella, Metalloporphyrins catalized oxidations, Kluwer Academic Publishers, Dordrecht, 1994.

[2] R.A. Sheldon, Metalloporphyrins in catalytic oxidations, Marcel Dekker, Inc., New York, 1994.

[3] B. Meunier, A. Robert, G. Pratviel, J. Bernadou, in: K.M. Kadish, K.M. Smith, R. Guilard (Eds.), Academic Press, 2000, p. 119.

[4] J.T. Groves, in: P.R. Ortiz de Montellano (Ed.), Cytochrome P-450: Structure, Mechanism, and Biochemistry, 3rd edition, Kluwer Academic/Plenum Publishers, New York, 2005, Chapter 1.

[5] D. Mansuy, C. R. Chim. 10 (2007) 392-413.

[6] F.P. Guengerich, C.D. Sohl, G. Chowdhury, Arch. Biochem. Biophys. 507 (2011) 126-134.

[7] S. Rendic, F.P. Guengerich, Chem. Res. Toxicol. 25 (2012) 1316-1383.

[8] J. Bernadou, B. Meunier, Adv. Synth. Catal. 346 (2004) 171-184.

[9] M.M.Q. Simões, R. De Paula, M.G.P.M.S. Neves, J.A.S. Cavaleiro, J. Porphyrins Phthalocyanines 13 (2009) 589-596.

[10] M.M.Q. Simões, C.M.B. Neves, S.M.G. Pires, M.G.P.M.S. Neves, J.A.S. Cavaleiro, Pure Appl. Chem. 85 (2013) 1671-1681.

[11] R. De Paula, M.M.Q. Simões, M.G.P.M.S. Neves, J.A.S. Cavaleiro, Evaluation of Five-Membered Heterocyclic Ring *meso*-Substituted Metalloporphyrins as Catalysts in Oxidative Reactions, 4th Spanish-Portuguese-Japanese Organic Chemistry Symposium, Santiago de Compostela/Spain, 2006, PO-26, p. 86.

[12] R. De Paula, M.M.Q. Simões, M.G.P.M.S. Neves, J.A.S. Cavaleiro, J. Mol. Catal. A: Chem. 345 (2011) 1-11.

[13] R.S. Czernuszewicz, Y.O. Su, M.K. Stern, K.A. Macor, D. Kim, J.T. Groves, T.G. Spiro, J. Am. Chem. Soc. 110 (1988) 4158-4165.

[14] J.T. Groves, Z. Gross, M.K. Stern, Inorg. Chem. 33 (1994) 5065-5072.

[15] W. Nam, I. Kim, M.H. Lim, H.J. Choi, J.S. Lee, H.G. Jang, Chem. Eur. J. 8 (2002) 2067-2071.

[16] J.R.L. Smith, Y. Iamamoto, F.S. Vinhado, J. Mol. Catal. A: Chem. 252 (2006) 23-30.

[17] N. Jin, M. Ibrahim, T.G. Spiro, J.T. Groves, J. Am. Chem. Soc. 129 (2007) 12416-12417.

[18] Y. Watanabe, H. Nakajima, T. Ueno, Acc. Chem. Res. 40 (2007) 554-562.

[19] J.F. Hull, D. Balcells, E.L.O. Sauer, C. Raynaud, G.W. Brudvig, R.H. Crabtree, O. Eisenstein, J. Am. Chem. Soc. 132 (2010) 7605-7616.

[20] T.P. Umile, D. Wang, J.T. Groves, Inorg. Chem. 50 (2011) 10353-10362.

[21] S.L.H. Rebelo, M.M. Pereira, M.M.Q. Simões, M.G.P.M.S. Neves, J.A.S. Cavaleiro, J. Catal. 234 (2005) 76-87.

[22] S.L.H. Rebelo, M.M.Q. Simões, M.G.P.M.S. Neves, A.M.S. Silva, J.A.S. Cavaleiro, Chem. Commun. (2004) 608-609.

[23] N.A. Stephenson, A.T. Bell, J. Am. Chem. Soc. 127 (2005) 8635-8643.

[24] R. De Paula, M.M.Q. Simões, M.G.P.M.S. Neves, J.A.S. Cavaleiro, Catal. Commun. 10 (2008) 57-60.

[25] Y. Iamamoto, M.D. Assis, K.J. Ciuffi, C.M.C. Prado, B.Z. Prellwitz, M. Moraes, O.R. Nascimento, H.C. Sacco, J. Mol. Catal. A: Chem. 116 (1997) 365-374.

[26] S.L.H. Rebelo, M.M.Q. Simões, M.G.P.M.S. Neves, A.M.S. Silva, J.A.S. Cavaleiro, A.F. Peixoto, M.M. Pereira, M.R. Silva, J.A. Paixão, A.M. Beja, Eur. J. Org. Chem. (2004) 4778-4787.

[27] P. Tagliatesta, D. Giovannetti, A. Leoni, M.G.P.M.S. Neves, J.A.S. Cavaleiro, J. Mol. Catal. A: Chem. 252 (2006) 96-102.

[28] S.M.G. Pires, R.D. Paula, M.M.Q. Simões, A.M.S. Silva, M.R.M. Domingues, I.C.M.S. Santos, M.D. Vargas, V.F. Ferreira, M.G.P.M.S. Neves, J.A.S. Cavaleiro, RSC Advances 1 (2011) 1195-1199.

[29] C.M.B. Neves, M.M.Q. Simões, M.R.M. Domingues, I.C.M.S. Santos, M.G.P.M.S. Neves, F.A.A. Paz, A.M.S. Silva, J.A.S. Cavaleiro, RSC Advances 2 (2012) 7427-7438.

[30] S.M.G. Pires, M.M.Q. Simões, I.C.M.S. Santos, S.L.H. Rebelo, M.M. Pereira, M.G.P.M.S. Neves, J.A.S. Cavaleiro, Appl. Catal. A: Gen. 439–440 (2012) 51-56.

[31] M. Linhares, S.L.H. Rebelo, M.M.Q. Simões, A.M.S. Silva, M.G.P.M.S. Neves, J.A.S. Cavaleiro, C. Freire, Appl. Catal. A: Gen. 470 (2014) 427-433.

[32] C.M.B. Neves, M.M.Q. Simões, I.C.M.S. Santos, F.M.J. Domingues, M.G.P.M.S. Neves, F.A.A. Paz, A.M.S. Silva, J.A.S. Cavaleiro, Tetrahedron Lett. 52 (2011) 2898-2902.

[33] S.L.H. Rebelo, M. Linhares, M.M.Q. Simões, A.M.S. Silva, M.G.P.M.S. Neves, J.A.S. Cavaleiro, C. Freire, J. Catal. 315 (2014) 33-40.

[34] S.M.G. Pires, M.M.Q. Simões, I.C.M.S. Santos, S.L.H. Rebelo, F.A.A. Paz, M.G.P.M.S. Neves, J.A.S. Cavaleiro, Appl. Catal. B: Environ. 160-161 (2014) 80-88.

[35] J. Poltowicz, E.M. Serwicka, E. Bastardo-Gonzalez, W. Jones, R. Mokaya, Appl. Catal. A: Gen. 218 (2001) 211-217.

[36] S. Tangestaninejad, M.H. Habib, V. Mirkhani, M. Moghadam, J. Chem. Res. S (2001) 444-445.

[37] E. Brulé, Y.R. Miguel, Org. Biomol. Chem. 4 (2006) 599-609.

[38] R. Rahimi, S.Z. Ghoreishi, M.G. Dekamin, Monatsh. Chem. 143 (2012) 1031-1038.

[39] S. Nakagaki, G.K.B. Ferreira, A.L. Marcal, K.J. Ciuffi, Curr. Org. Synth. 11 (2014) 67-88.

[40] K.A.D.F. Castro, M.M.Q. Simões, M.G.P.M.S. Neves, J.A.S. Cavaleiro, F. Wypych, S. Nakagaki, Catal. Sci. Technol. 4 (2014) 129-141.

[41] S.L.H. Rebelo, A.R. Gonçalves, M.M. Pereira, M.M.Q. Simões, M.G.P.M.S. Neves, J.A.S. Cavaleiro, J. Mol. Catal A: Chem. 256 (2006) 321-323.

[42] S.M.G. Pires, R. De Paula, M.M.Q. Simões, M.G.P.M.S. Neves, I.C.M.S. Santos, A.C. Tomé, J.A.S. Cavaleiro, Catal. Commun. 11 (2009) 24-28.

[43] M. Moghadam, S. Tangestaninejad, M.H. Habibi, V. Mirkhani, J. Mol. Catal. A: Chem. 217 (2004) 9-12.

[44] C.P. Du, Z.K. Li, X.M. Wen, J. Wu, X.Q. Yu, M. Yang, R.G. Xie, J. Mol. Catal. A: Chem. 216 (2004) 7-12.

[45] J.Y. Liu, X.F. Li, Y.Z. Li, W.B. Chang, A.J. Huang, J. Mol. Catal. A: Chem. 187 (2002) 163-167.

[46] P. Anzenbacher, V. Kral, J. Mol. Catal. A: Chem. 96 (1995) 311-315.

[47] D. Kumar, S.P. de Visser, S. Shaik, Chem. Eur. J. 11 (2005) 2825-2835.

[48] A.N. de Sousa, M. de Carvalho, Y.M. Idemori, J. Mol. Catal. A: Chem. 169 (2001) 1-10.

[49] A.J. Appleton, S. Evans, J.R.L. Smith, J. Chem. Soc. Perkin Trans. 2 (1996) 281-285.

[50] I.C.M.S. Santos, M.M.Q. Simões, M.M.M.S. Pereira, R.R.L. Martins, M.G.P.M.S. Neves, J.A.S. Cavaleiro, A.M.V. Cavaleiro, J. Mol. Catal. A: Chem. 195 (2003) 253-262.

[51] J.R. Lindsay-Smith, in: R.A. Sheldon (Ed.), Metalloporphyrins in catalytic oxidations, Marcel Dekker, Inc., New York, 1994, chapter 11.

[52] R. De Paula, PhD Thesis, Department of Chemistry, University of Aveiro, 2009.

[53] M. Gouterman, in: D. Dolphin (Ed.), The Porphyrins, Academic Press, New York, 1978, p. 1-165.

[54] N. Jin, J.T. Groves, J. Am. Chem. Soc. 121 (1999) 2923-2924.

[55] F. De Angelis, N. Jin, R. Car, J.T. Groves, Inorg. Chem. 45 (2006) 4268-4276.

[56] R. De Paula, M.A.F. Faustino, D.C.G.A. Pinto, M.G.P.M.S. Neves, J.A.S. Cavaleiro, J. Heterocycl. Chem. 45 (2008) 453-459.

[57] D.H. Tjahjono, T. Akutsu, N. Yoshioka, H. Inoue, Biochim. Biophys. Acta-Gen. Subj. 1472 (1999) 333-343.